Journal of Physics: Conference Series

**PAPER** • **OPEN ACCESS**

# A new method for estimating pollutant concentration in unsaturated soil using digital image processing technique

To cite this article: N Soleimanian and A Akhtarpour 2021 *J. Phys.: Conf. Ser.* **1973** 012204

View the article online for updates and enhancements.


This content was downloaded from IP address 94.130.124.126 on 02/09/2021 at 08:28

# A new method for estimating pollutant concentration in unsaturated soil using digital image processing technique

**N Soleimanian[1], A Akhtarpour[2]**
[1]PhD Student, Department of Civil Engineering, Faculty of Engineering, Ferdowsi University of Mashhad, Iran
[2]Associate Professor, Department of Civil Engineering, Faculty of Engineering, Ferdowsi University of Mashhad, Iran, ORCID: 0000-0003-1654-0194

E-mail: narges.soleimanian@mail.um.ac.ir, akhtarpour@um.ac.ir

**Abstract.** In recent decades, the vast potential of entry of solid waste and landfill leachate in soil and groundwater has caused pollutant emission, and concentration in-depth become an important issue. In order to clean or prevent soil contamination, the emission and concentration of the pollutant in soil should be specified. In this study, the digital image processing technique as a new method is used to determine the pollutant concentration in soil depth. In this regard, at first, several experimental tests are done. Then, the image processing technique and numerical simulation are utilized to determine the concentration of pollutants. Experimental test results validate the results of the finite element simulation. The results indicate a good agreement between the image processing method and numerical analyses in estimating concentration. Therefore, the image processing technique can be used as a simple, useful, and time-effective method for estimating concentration in unsaturated soil.

## 1. Introduction

Digital image processing is a new science that goes back to the invention of digital computers. However, this new science has made significant progress in recent decades, both theoretically and practically. The digital image processing (D.I.P) technique is used in many fields of civil engineering. For example, digital image processing technique was used to evaluate the stress situation in the pavement, measure the morphological parameters of the materials, reveal physical properties of materials (grain size), study the crack propagation process and the patterns of material fracture [1,2,3,4,5].

In addition, D.I.P.-based methods were utilized to detect rock slope motion [6], measurement of the dynamic movement of building [7], pollutant concentration approximation [8,9]. Also, digital image processing method has been applied in various areas for advanced infrastructure inspections and assessment [10].

Based on research done, some studies have been done on contaminant emission [11,12,13,14] but no comprehensive research has been conducted on estimating pollutant concentration in the soil. The innovation of this study is the use of an image processing method to estimate the concentration of pollutants in the unsaturated soil. Given the importance of the environment and the protection of groundwater resources, this method can be efficient and useful for estimating concentration and providing methods to prevent the infiltration of pollutants into groundwater.

In this study, MATLAB software is used for image processing and Average and Median filters are utilized to remove the noise and enhance the image restoration [15]. The average filter improves the pixel value of an image by the average grayscale in the neighborhood. It is a simple, intuitive, and easy

Content from this work may be used under the terms of the Creative Commons Attribution 3.0 licence. Any further distribution of this work must maintain attribution to the author(s) and the title of the work, journal citation and DOI.
Published under licence by IOP Publishing Ltd

to implement a technique to improve the image by reducing image pixel intensity changes. It is often used to smooth and blur the image, to reduce noise in images [16]. Medium filtering is a nonlinear method used to remove noise from images based on statistics. It retains this useful image information, and the original pixel gray value is converted to the gray pixel values in a particular neighborhood. This filter reduces the noise of an image without blurring the edges of the image. The average is calculated by sorting all the neighborhood window pixel values numerically and replacing the intended pixel with the value of the middle pixel, respectively [17].

## 2. Materials and methods

To achieve the objectives of this research, a series of experimental and numerical studies were performed, the explanations of which are presented below.

### *2.1. Experimental model*

In this study, a glass rectangular cube model with dimensions of 120 × 8 × 80 centimeters was constructed to estimate the concentration of pollutants in-depth in unsaturated soil (Fig.1). The reason for the low thickness of this model was better to photograph the emission of pollutants in the soil. The soil used in this experiment was the 131 standard Firoozkooh sand, and its specifications are given in Table 1.

After filling the soil box up to 60 cm, the bottom valves of the box, which is shown in Fig. 1, were opened, and the soil was completely saturated (The valves under the model are designed for water inlet and outlet). After saturation, the box was left for 24 hours to remove all air bubbles. Then, by opening the bottom valves, the surface of the water was brought down to a height of approximately 10 cm from the bottom of the box. Penetration of the pollutant was performed after 48 hours to balance the relative humidity inside the soil. Tests for soil with densities of 60, 80, and 100% have been performed.

In this study, leachate was used as a contaminant that had the same composition in each experiment (absolute weight of fat, protein, carbohydrate and fiber) due to the reproducibility of the experiments. Red was used to better see the transfer of leachate to the soil. The pollutant was penetrated in the soil by a glass rectangle cube with dimensions 3×7×20 centimeters and a constant head (3 cm). The test continued until the pollutant arrived at the bottom of the box, and photos were taken during pollutant propagation at 5, 50, and 150 seconds.

**Table 1.** Specifications of the 131 standard Firoozkooh sand.

| $e_{max}$ | $e_{min}$ | $G_s$ | $D_{50}$ | $D_{10}$ | $D_{60}$ |
|---|---|---|---|---|---|
| 1.091 | 0.71 | 2.656 | 0.65 | 0.45 | 0.67 |

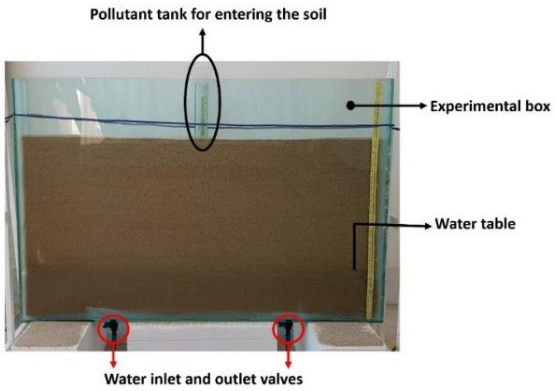


**Figure 1.** Experimental model.

### *2.2. Numerical Analysis*

#### *2.2.1. Modeling in SEEP/W software*

In the Geostudio2012 package, Density-Dependent Analysis should be used to analyze emissions of pollutants with various densities. In order to investigate the emission of pollution in a porous medium such as soil, a model should be constructed in the SEEP/W, which main task is to express the hydraulic conditions of the area under investigation. In this research, saturated permeability was measured by constant head tests, and the characteristics of the SWCC curve were also estimated by soil aggregation. A two-dimensional and square mesh with 9 Gaussian points for mesh studies were used. For entering pollutant, boundary condition with the constant head was considered [18].

#### *2.2.2. Modeling in CTRAN/W software*

The model made in the SEEP/W package was transferred to the CTRAN/W to simulate pollutant emission. For this purpose, the pollutant functions' characteristics, including diffusion, longitudinal dispersion, transverse dispersion, and soil properties, should be determined. The amount of diffusion coefficient was considered according to the studies by Kuo [19]. It should be noted that according to the Geostudio2012 documentation, the longitudinal dispersion coefficient in laboratory tests is generally equal to 0.1 of the length of laboratory model dimensions. The transverse dispersion coefficient should also be assumed to be less than the longitudinal dispersion coefficient and about half of it. Finally, boundary conditions of the pollutant entry in the soil defined constant concentration (1 g/m3). Tables 2 and 3 show the parameters used in SEEP/W and CTRAN/W models.

**Table 2.** Soil properties used in the numerical models.

| **The density of sand (%)** | **Permeability (m/s)** | **Porosity** |
|---|---|---|
| 40 | 0.00061 | 0.481 |
| 60 | 0.0005 | 0.458 |
| 80 | 0.00041 | 0.434 |
| 100 | 0.00033 | 0.403 |

**Table 3.** Models' specifications.

| **Parameter** | **Unit** | **Value** |
|---|---|---|
| The relative density of pollutant | - | 1.2 |
| Pollutant head | cm | 3 |
| The water level of groundwater | cm | 10 |
| Longitudinal Dispersivity | m | 0.12 |
| Transverse Dispersivity | m | 0.06 |
| Diffusion | $m^2/s$ | $10^{-9}$ |
| Time | s | 400 |
| Width of the model | cm | 60 |
| Length of the model | cm | 120 |

### *2.3. Image processing*

Coding in MATLAB software was used for image analysis. In this process, images taken from the emission of pollutants into the soil were inputs for software and the curves showing the variation of color intensity versus the pixels in-depth of the soil were the outputs. At first, an initial image of the

test box and the lighting condition was taken before the leakage event. After that, taking images were repeated at each stage (various densities of soil) of the leakage at different times (5, 50 and, 150 seconds). It was important to be careful that the light condition was the same for all the images. In this study, images were examined in gray color space. A wide range of colors from white to black was assigned to the numbers 0 to 255. In this range, 0 shows the black, and 255 shows the white.
Initially, the images were in red, green and blue colors (RGB) space. Then, the RGB image was converted to a gray image. For this purpose, the binary format of the image was used as a filter on the initial image in RGB color space. After that, the image was transferred to hue, saturation and lightness (HSV) color space in the value band. Fig. 2 shows the HSV and RGB space. Average and median filters were used to reduce image noise. Fig. 3 shows the function of the filter image processing algorithm. Therefore, the curve of color intensity changes versus pixels in-depth was plotted in the middle of the area of pollutant emission. After that, it should be converted to a concentration curve versus depth. For this regard, the highest color intensity of each curves was given 100% concentration, and the lowest color intensity for each curve was given 0% concentration. Because of the existing noise in each curve, it is necessary to fit it into a linear function to compare it with the concentration curves from the finite element analysis (FEA). The curve of concentration change relative to the depth is presented by Geostudio2012 software, as shown in Fig 4.

## 3. Results and conclusion

### *3.1. Comparison between experimental modeling and numerical analysis*

Numerical modeling for pollutant emissions was performed following laboratory modeling. The penetration depth of the pollutant into the soil at different times was compared in the numerical and laboratory models. Figure 5 shows an example of numerical modeling for soil with a density of 100% and 50 seconds after emission beginning (The D parameter shows the penetration depth). According to Fig. 6, the Numerical model has good consistency with laboratory model results. The results showed that the numerical model was well able to simulate the emission of pollutants in the soil. So, it is an efficient model to estimate the concentration of pollutants and compare it with the image processing method.

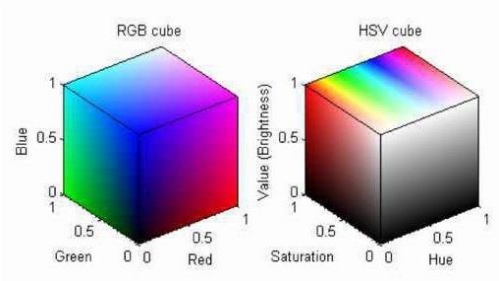


**Figure 2.** HSV and RGB space.

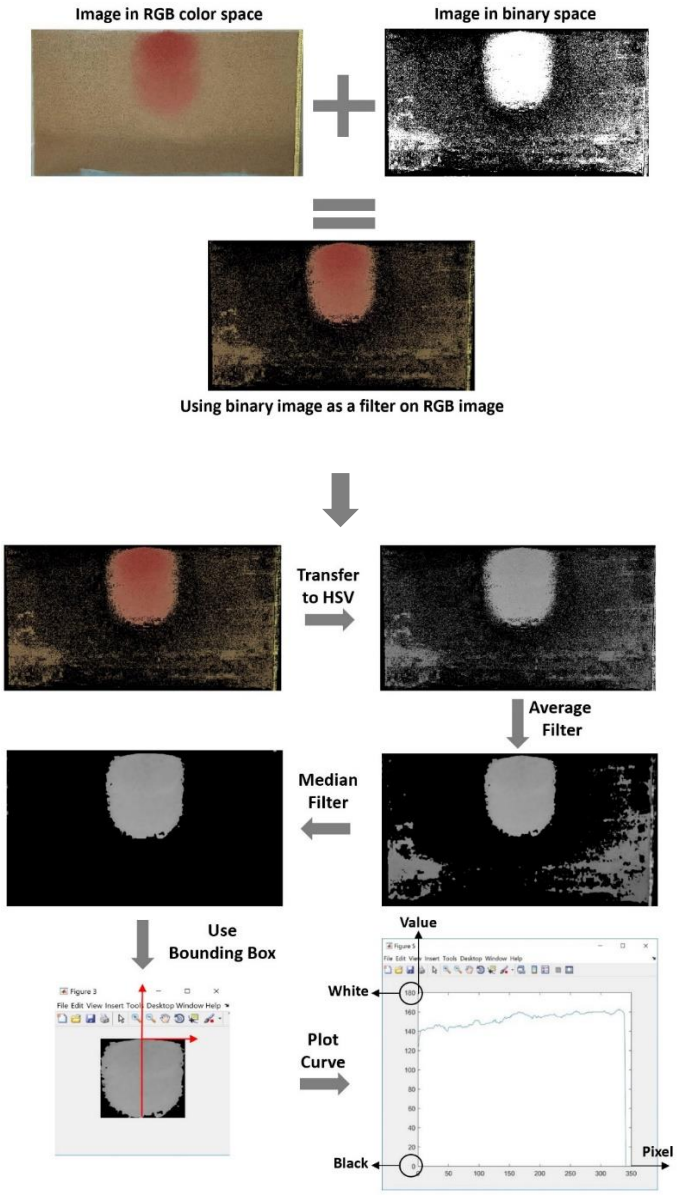


**Figure 3.** Function of image processing algorithm.

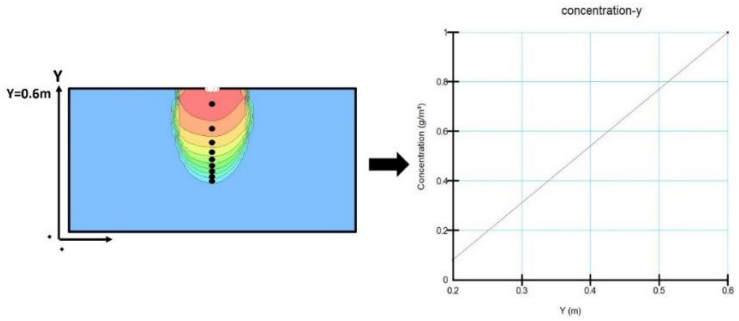


**Figure 4.** The curve for the variation of concentration based on elevation from bottom of FEA.

**a) Numerical model. D=19cm** **b) Laboratory model. D=19cm**

**Figure 5.** Comparison between pollution emission in the laboratory and numerical model in unsaturated soil with 100% density after 50 second.

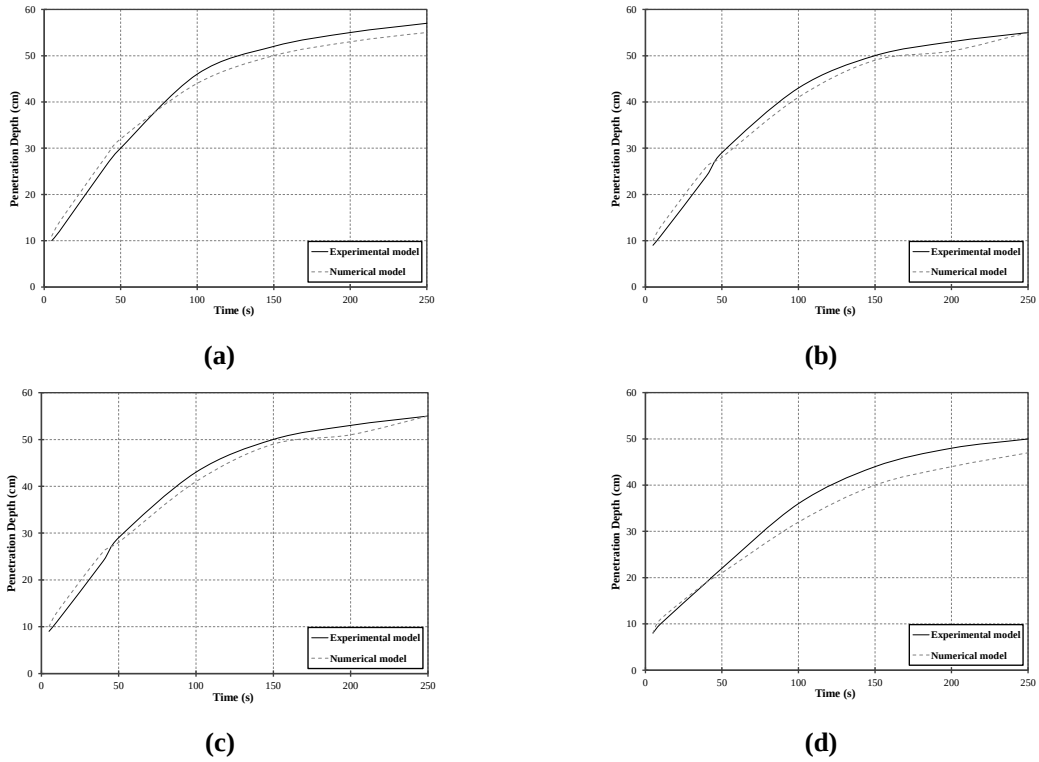


**Figure 6.** Curve for the comparison of the results of FEA and laboratory test in unsaturated soil for densities: a) 40%, b) 60%, c) 80%, and d) 100%.

*3.2. Image processing*

In this section, for images taken from the emission of pollutants into the soil at 5, 50, and 150 seconds at all densities, the concentration curve was plotted and compared with the results of Geostudio2012 software.

Fig. 7 to 9 show the concentration curve obtained from image analysis and FEA for sandy soils with the density of 60%, 80%, and 100%, and the results of the comparison are presented in Tables 5, 6 and, 7. Given that, for sandy soils with a density of 60%, the pollutant has penetrated to groundwater in 150 seconds, two concentration curves were drawn. One chart was shown concentration changes in depth from soil surface until the groundwater level, and the other was examined changes in concentration until the depth of pollutant penetration.

As shown in the curves, the concentration curves obtained from image analysis and FEA have the same decline rate. They can estimate the concentration of pollutants in the soil with a negligible percentage

of error. By increasing soil density, the difference between the curves obtained from image analysis and software decreases. By entering the pollutant into the groundwater, due to the difference in the background color of the photo in the soil saturation region, the intensity of the pollutant color becomes more, and image analysis cannot predict the concentration well. Therefore, it is suggested that the changes in concentration to the groundwater level boundary be examined.
The results show that, this research has good accuracy. Given the importance of the environment and the protection of groundwater resources, this method can be efficient and useful for estimating concentration and providing methods to prevent the infiltration of pollutants into groundwater.

**Table 4.** Results obtained from the comparison of concentration curve in FEA and image analysis in soil with 60% density.

| Time (s) | Rate of concentration decrease in-depth (image analysis) | Rate of concentration decrease in-depth (FEA) | Percent average error from the prediction of the concentration by image analysis |
|---|---|---|---|
| 5 | 0.106 | 0.1 | 4% |
| 50 | 0.041 | 0.038 | 5% |
| 150 (to the level of water table) | 0.025 | 0.025 | 9% |

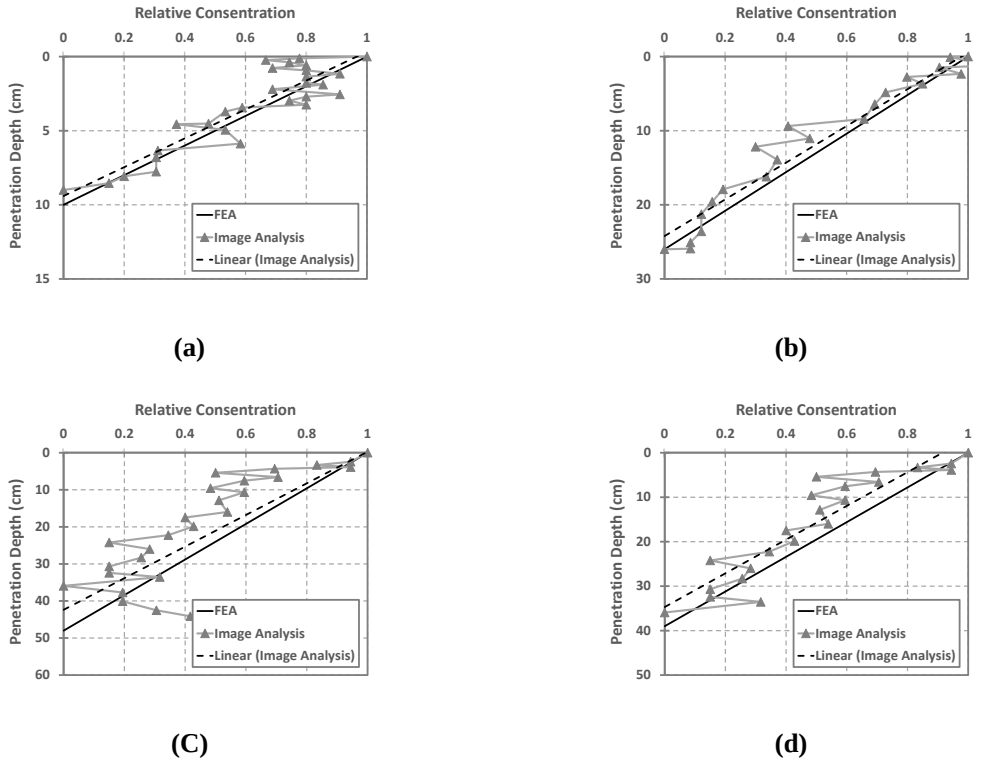


**Figure 7.** Comparison of concentration curve in FEA and image analysis in soil with 60% density in a) 5 s, b) 50 s, c) 150 s, d) 150 s (to the level of groundwater).

**Table 5.** Results obtained from the comparison of concentration curve in FEA and image analysis in soil with 80% density.

| Time (s) | Rate of concentration decrease in-depth (image analysis) | Rate of concentration decrease in-depth (FEA) | Percent average error from the prediction of the concentration by image analysis |
|---|---|---|---|
| 5 | 0.142 | 0.142 | 2% |
| 50 | 0.04 | 0.04 | 5% |
| 150 | 0.022 | 0.023 | 4% |

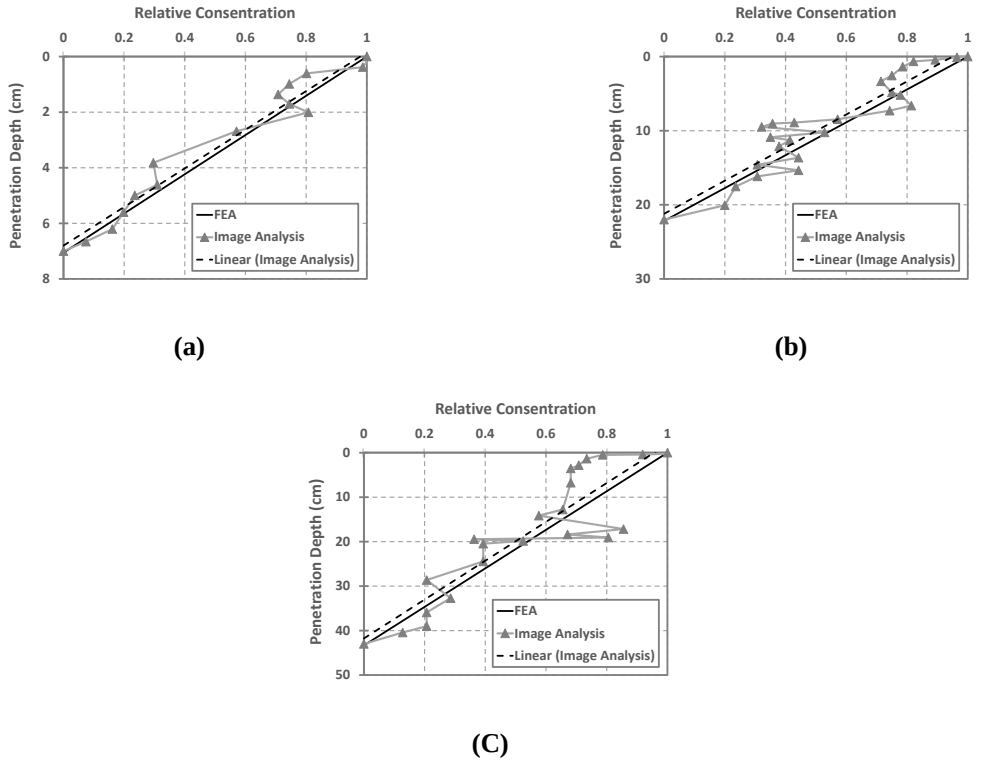


**Figure 8.** Comparison of concentration curve in FEA and image analysis in soil with 80% density in a) 5 s, b) 50 s, c) 150 s.

**Table 6.** Results obtained from the comparison of concentration curve in FEA and image analysis in soil with 100% density.

| Time (s) | Rate of concentration decrease in-depth (image analysis) | Rate of concentration decrease in-depth (FEA) | Percent average error from the prediction of the concentration by image analysis |
|---|---|---|---|
| 5 | 0.17 | 0.166 | 1% |
| 50 | 0.051 | 0.052 | 1% |
| 150 | 0.026 | 0.027 | 1% |

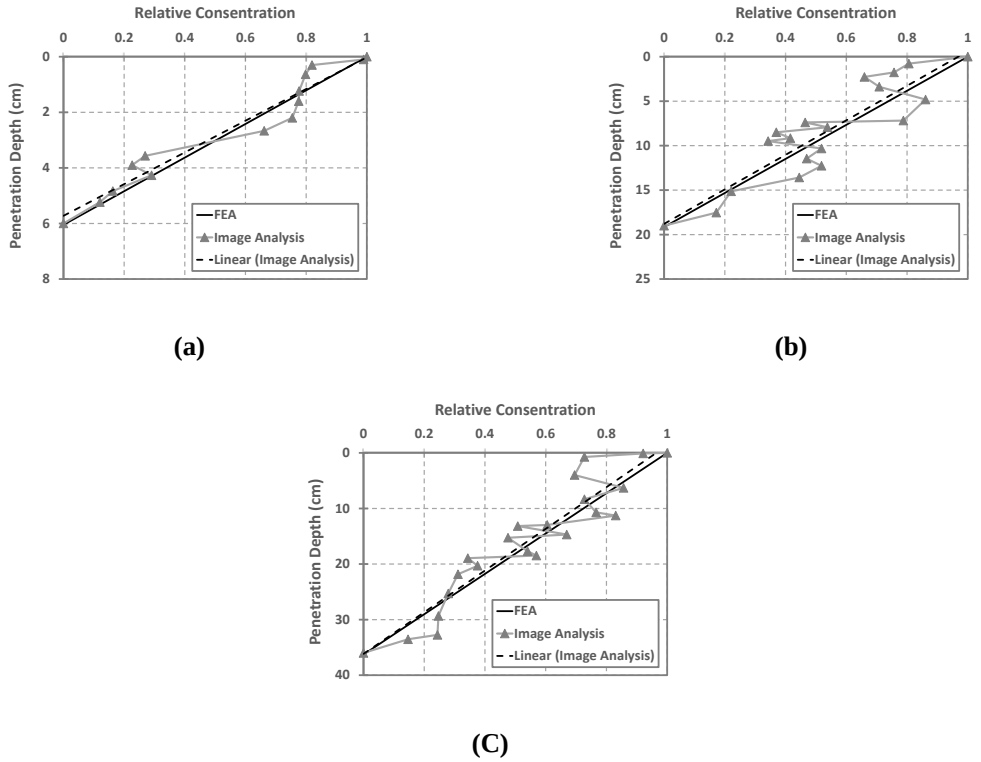


**Figure 9.** Comparison of concentration curve in FEA and image analysis in soil with 100% density in a) 5 s, b) 50 s, c) 150 s.

## 4. References

[1] Persson AL. Image analysis of shape and size of fine aggregates. Engineering Geology. 1998 Sep 1;50(1-2):177-86.

[2] Ghalib AM, Hryciw RD. Soil particle size distribution by mosaic imaging and watershed analysis. Journal of Computing in Civil Engineering. 1999 Apr;13(2):80-7.

[3] Diamond S, Huang J. The ITZ in concrete–a different view based on image analysis and SEM observations. Cement and concrete composites. 2001 Apr 1;23(2-3):179-88.

[4] Peterson KW, Swartz RA, Sutter LL, Van Dam TJ. Hardened concrete air void analysis with a flatbed scanner. Transportation Research Record. 2001;1775(1):36-43.

[5] Reid TR, Harrison JP. A semi-automated methodology for discontinuity trace detection in digital images of rock mass exposures. International Journal of Rock Mechanics and Mining Sciences. 2000 Oct 1;37(7):1073-89.

[6] Corthèsy R, Leite M.H. Digital imaging for rock slope movement detection. In processing of the 12th Panamerican Conference for soil mechanics and Geotechnical Engineering and the 39th US rock Mechanics Symposium, Soil and Rock America 2003. MIT, Boston, USA. 2003 June;185-192.

[7] Ferrer B, Espinosa J, Roig AB, Perez J, Mas D. Vibration frequency measurement using a local multithreshold technique. Optics express. 2013 Nov 4;21(22):26198-208.

[8] Epitropou V, Karatzas KD, Bassoukos A, Kukkonen J, Balk T. A new environmental image processing method for chemical weather forecasts in Europe. InInformation Technologies in Environmental Engineering 2011 (pp. 781-791). Springer, Berlin, Heidelberg.

[9] Moropoulou A, Koui M, Kourteli C, Achilleopoulos N, Zezza F. Digital Image Processing for Weathering Analysis and Planning of Conservation Interventions on Historic Structures and Complexes. InAdvances in Intelligent Systems 1999 (pp. 401-414). Springer, Dordrecht.

[10] Li L, Lee P.KK, Tsui Y, Tham L.G, Tang C.A. Failure process of granite. International Journal of Geomechanics. A.S.C.E. 2003;3(1): 84-98.
[11] Alsamia SM, Mahmood MS, Akhtarpour A. Prediction of the contamination track in Al-Najaf city soil using numerical modelling. InIOP Conference Series: Materials Science and Engineering 2020 Jul 1 (Vol. 888, No. 1, p. 012050). IOP Publishing.
[12] Alsamia S, Mahmood MS, Akhtarpour A. Estimation of capillary rise in unsaturated gypseous sand soils. Pollack Periodica. 2020 Aug;15(2):118-29.
[13] Qu M, Li W, Zhang C, Huang B, Zhao Y. Estimating the pollution risk of cadmium in soil using a composite soil environmental quality standard. The Scientific World Journal. 2014 Jan 1;2014.
[14] Chen TB, Zheng YM, Lei M, Huang ZC, Wu HT, Chen H, Fan KK, Yu K, Wu X, Tian QZ. Assessment of heavy metal pollution in surface soils of urban parks in Beijing, China. Chemosphere. 2005 Jul 1;60(4):542-51.
[15] Maheshan CM, Kumar HP. Performance of image pre-processing filters for noise removal in transformer oil images at different temperatures. SN Applied Sciences. 2020 Jan 1;2(1):67.
[16] Jayaraman S, Esakkirajan S, Veerakumar T. Digital image processing. Tata McGraw Hill, New York. 2011.
[17] Lee Y, Kassam S. Generalized median filtering and related nonlinear filtering techniques. IEEE Transactions on Acoustics, Speech, and Signal Processing. 1985 Jun;33(3):672-83.
[18] Lu N, Likos WJ. Suction stress characteristic curve for unsaturated soil. Journal of geotechnical and geoenvironmental engineering. 2006 Feb;132(2):131-42.
[19] Kuo J. Practical design calculations for groundwater and soil remediation. CRC Press; 2014 Jun 2.